Signaling pathway of morphine induced acute thermal hyperalgesia in mice.

Pain 123 (2006) 294–305

PAIN

www.elsevier.com/locate/pain

Signaling pathway of morphine induced acute thermal hyperalgesia in mice

Nicoletta Galeotti [a], George B. Stefano [b], Massimo Guarna [c], Enrica Bianchi [d,*], Carla Ghelardini [a]

[a] *Department of Clinical and Preclinical Pharmacology, University of Florence, Florence, Italy*
[b] *Neuroscience Research Institute, State University of New York, NY, USA*
[c] *Department of Biomedical Sciences, University of Siena, Siena, Italy*
[d] *Department of Neuroscience, University of Siena, Siena, Italy*

Received 26 August 2005; received in revised form 20 February 2006; accepted 13 March 2006

Abstract

Systemic administration of morphine induced a hyperalgesic response in the hot plate test, at an extremely low dose (1–10 μg/kg). We have examined in vivo whether morphine, at an extremely low dose, induces acute central hypernociception following activation of the opioid receptor-mediated PLC/PKC inositol-lipid signaling pathway. The PLC inhibitor U73122 and the PKC blocker, calphostin C, dose dependently prevented the thermal hypernociception induced by morphine. This effect was also prevented by pretreatment with aODN against PLCβ$_3$ at 2 nmol/mouse and PKCγ at 2–3 nmol/mouse. Low dose morphine hyperalgesia was dose dependently reversed by selective NMDA antagonist MK801 and ketamine. This study demonstrates the presence of a nociceptive PLCβ$_3$/PKCγ/NMDA pathway stimulated by low concentrations of morphine, through μOR$_1$ receptor, in mouse brain. This signaling pathway appears to play an opposing role in morphine analgesia. When mice were treated with a morphine analgesic dose (7 mg/kg), the downregulation of PLCβ$_3$ or PKCγ at the same aODN doses used for the prevention of the hyperalgesic effect induced, respectively, a 46% and 67% potentiation in analgesic response. Experimental and clinical studies suggest that opioid may activate pronociceptive systems, leading to pain hypersensitivity and short-term tolerance, a phenomenon encountered in postoperative pain management by acute opioid administration. The clinical management of pain by morphine may be revisited in light of the identification of the signaling molecules of the hyperalgesic pathway.

Keywords: Morphine; Hyperalgesia; Opioid receptor; Phospholipase β; Protein kinase Cγ; NMDA receptor

1. Introduction

A growing body of evidence suggests that μOR opioid agonists induce not only analgesia, but may also enhance sensitivity to pain. This paradoxical effect has been demonstrated both in clinical (Guignard et al., 2000; Angst et al., 2003; Compton et al., 2003) and laboratory studies (Laulin et al., 1998; Celerier et al., 1999, 2000, 2001; Laulin et al., 2002; Van Elstraete et al., 2005). Morphine, at higher doses, induces analgesia. The alkaloid, via opioid receptors and PTX sensitive inhibitory G protein (G_i), inhibits cyclic AMP (cAMP) formation, Ca^{2+} conductance and activates K^+ conductance leading to hyperpolarization of a cell and exerting an inhibitory effect (Nestler, 1992). Otherwise, extremely low doses of morphine (1–10 μg/kg) can elicit acute hyperalgesia in animal models of pain, i.e., tail flick, Freund's adjuvant-induced arthritic rats (Kayan et al.,

Abbreviations: aODN, antisense phosphodiester oligonucleotide; DAG, 1,2-diacylglycerol; NMDA, *N*-methyl-D-aspartate; PKCγ, protein kinase Cγ; PLCβ, phospholipase Cβ

* Corresponding author. Tel.: +39 677 234151.
E-mail address: bianchi16@unisi.it (E. Bianchi).

0304-3959/$32.00
doi:10.1016/j.pain.2006.03.008

1971; Kayser et al., 1987; Crain and Shen, 2001). A dual effect of opioids on cAMP formation was reported in cell culture. A low concentration (10^{-9} M) of DAMGO, a selective μOR agonist, stimulated cAMP production, while a higher concentration (10^{-7} M) of the agonist inhibited cAMP production (Rubovitch et al., 2003). Stimulatory effect of a single administration of opioids at very low doses in dorsal root ganglion isolated cells has been demonstrated to be mediated by coupling of opioid receptors to cholera toxin sensitive second excitatory messenger proteins (Crain and Shen, 1998). Others have reported in cultured cells stimulatory effects for opioid receptors, following coupling to G_i proteins that also mediate the better known inhibitory effects. The opioid-induced stimulatory effect leads to activation of PLC in various cell types via PTX sensitive G_i proteins (Smart et al., 1995; Tsu et al., 1995; Chan et al., 2000), triggering the activation of the phosphoinositide-signaling cascade (Smart and Lambert, 1996). Most importantly, opioid receptors have the ability to activate the PLCβ isoenzymes via the βγ subunit of G_i protein (Park et al., 1993), suggesting a role for these isoenzymes in morphine-induced hyperalgesia. In the phosphoinositide-signaling pathway, the activation of PLCβ results in the hydrolysis of phosphatidylinositol 4,5-bisphosphate (PIP_2) followed by the generation of two important second messengers, inositol 1,4,5-trisphosphate ($InsP_3$) and 1,2-diacylglycerol (DAG). The former increases the release of Ca^{2+} from intracellular stores and the latter activates protein kinase Cγ (PKCγ), one of the major PKC isoforms (Fig. 1). PKCγ has been identified in neurons of CNS and strongly modulates opioid-signaling efficacy triggering the activation of *N*-methyl-D-aspartate (NMDA) glutamatergic receptors and the recruitment of the glutamatergic NMDA systems involved in pain stimulation (Celerier et al., 1999, 2004; Sanchez-Perez and Felipo, 2005).

In the present report, we determined the signaling pathway involved in the brain mechanisms associated with low dose morphine-induced hyperalgesia in mice. In this regard, we used supraspinal administration of activators, inhibitors and antisense phosphodiester oligonucleotides (aODNs) against the main signaling components of the nociceptive pathway in order to determine which messenger molecules are responsible for the change in nociceptive thermal threshold after systemic morphine administration in mice.

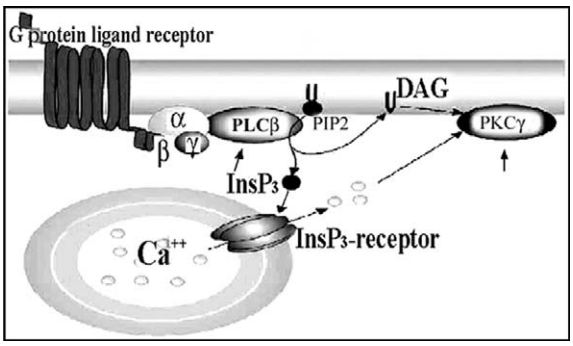

Fig. 1. PLC/PKC inositol-lipid signaling pathway is represented in the scheme.

2. Materials and methods

2.1. Animals

Sexually mature male Swiss Webster mice (Morini, S. Polo d'Enza, Italy), weighing 23–30 g, were used. The animals were fed a standard laboratory diet and water ad libitum, kept at 23 ± 1 °C with a 12-h light/dark cycle and previously habituated to the laboratory according to Abbott et al. (1986). All experiments were carried out in accordance with the European Community Council Directive of November 24 1986 for the care and use of laboratory animals.

2.2. Drugs

The following drugs were used: (*E*)-7-benzylidenenaltrexone tartrate (BNTX), D-Phe-Cys-Tyr-D-Trp-Orn-Thr-Pen-Thr-NHh2 (CTOP), forskolin, ketamine, morphine HCl, MK-801, naloxone, naloxone methiodide, naltriben, naloxonazine and norbinaltorphimine HCl (nor-NBI) (Sigma Chemicals, St. Louis, MO, USA); calphostin C, 1-[6-[[17β-3-methoxyestra-4,3,5(10)-trien-17-yl]amino]hexyl]1*H*-pyrrole-2,5-dione (U-73122) and 1-[6-[[17β-3-methoxyestra-1,3,5(10)-trien-17-yl]amino]hexyl]-1*H*-pyrrolidinedione (U-73343) (Calbiochem, Milan, Italy). Drugs were administered in a volume of 5 μl per mouse by intracerebroventricular (i.c.v.) injection, and 10 ml/kg by subcutaneous (s.c.) administration. Calphostin C, forskolin, U-73122 and U-73343 were dissolved in 0.5% DMSO, whereas all other drugs were dissolved in isotonic (NaCl 0.9%) saline solution immediately before use. Doses and administration schedules of substances applied in this study were based on doses shown to be effective in previous reports. Morphine was administered s.c. immediately prior estimation of hot plate licking latency (Glare and Walsh, 1991). Calphostin C was injected i.c.v. 60 min before morphine administration (Ghelardini et al., 2002); naltriben was administered i.c.v. 30 min prior morphine (Rawls et al., 2005); U-73122, U-73343, BNTX (Rady et al., 1994), ketamine (Ji et al., 2004) and MK-801 (Lee et al., 2002) were administered i.c.v. 10 min prior morphine; CTOP (Suh and Tseng, 1990), forskolin (Suh et al., 1996) and nor-NBI (Janecka et al., 2005) were injected i.c.v. immediately before morphine administration; naloxonazine was administered i.c.v. 24 h before morphine (Simone et al., 1986); naloxone (Jinsmaa et al., 2005) and naloxone methiodide (Wu et al., 1997) were administered s.c., respectively, 10 and 30 min before morphine administration.

2.3. Antisense oligodeoxynucleotides

Phosphodiester oligonucleotides (ODNs) protected by terminal phosphorothioate double substitution (capped ODNs) against possible exonuclease-mediated degradation were obtained from Tib Molbiol (Genoa, Italy). The following aODN was produced against PLCβ$_3$: 5′-T*GG*TGGTCATCT

GGGATG*T*A-3′ where * indicates the phosphorothioate residue. Anti-PLCβ$_3$ ODN was designed from the sequence 2649 to 2669 of the gi: 31982121 NCBI Sequence Wiewer; this sequence was searched through GenBank and found to be unique to its respective PLCβ$_3$ isoenzyme and was based on mouse sequence. The aODN against PKCγ was the following: 5′-A*C*GAAGTCCGGGTTCACA*T*A-3′. Anti-PKCγ ODN was designed from the sequence 2359 to 2378 of the gi: 31982442 NCBI Sequence Wiewer; this sequence was searched through GenBank and found to be unique to its respective PKCγ isoenzyme and was based on mouse sequence. Three base pairs in the antisense sequence were reversed to obtain the following mismatch sequence (mODNs): 5′-T*GG*TG *TG*CATC*GT*GG*TA*G*T*A-3′ and 5′-A*C*GA*GA*TC*GC*GG TT*AC*CA*T*A-3′ sequence, respectively, for PLCβ$_3$ and PKCγ isoenzymes. The 17 and 20mer fully degenerated ODNs (dODNs), where each base was randomly G, or C, or A, or T, were used as degenerate ODN (dODN). Antisense ODNs, mODNs and dODNs were preincubated at 37 °C for 30 min with an artificial cationic lipid (13 μM DOTAP, Sigma) and i.c.v. injected to mice in a 5 μl final volume of DOTAP according to a previously described method (Haley and McCormick, 1957). The ODNs were supplied to mice by i.c.v. injection 72, 48 and 24 h prior morphine administration.

2.4. Cyclic AMP determination

Mice were subcutaneously administered with 1 μg/kg or 7 mg/kg morphine or saline and sacrificed 15 or 30 min after morphine administration, at the time of the maximum thermal hyperalgesic effect according to behavioural studies. Liquid nitrogen frozen brain areas were obtained from mice and homogenized in 1 M acetic acid (1:2 w/v). After incubation in a 95 °C water bath for 15 min, brain tissue was centrifuged at 1500*g* for 15 min. Supernatant was homogenized in 5% trichloroacetic acid and centrifuged for 30 min at 3000*g* for 20 min at 4 °C. Supernatant fraction was trichloroacetic acid removed by extracting with three volumes of water saturated ethyl ether, adjusted to pH 6.2 and submitted to radioimmunoassay for cAMP according to Steiner (1974).

2.5. DAG determination

Mice were subcutaneously administered with 1 μg/kg morphine or saline and sacrificed 15 or 30 min after morphine administration. The extraction of DAG from mouse brain was carried out according to the method of Bligh and Dyer (1959). Liquid nitrogen frozen areas from both cerebral hemispheres of mouse brain were homogenized (1:10 w/v) with chloroform/methanol solution (1:2 v/v). A reagents system (Amersham Biosciences, USA) was used, based on a radioenzymatic assay employing diacylglycerol kinase quantitatively converting DAG to [^{32}P]phosphatidic acid in the presence of [γ-^{32}P]ATP. [^{32}P]Phosphatidic acid was separated on Amprep minicolumns and quantified using liquid scintillation spectrometry.

2.6. Hot plate test

The adopted method was previously described (O'Callaghan and Holtzman, 1975). Mice were placed inside a stainless steel container, which was set thermostatically at 52.5 ± 0.1 °C in a precision water bath from KW Mechanical Workshop, Siena, Italy. We used a lower temperature in the hot plate test (52.5 °C instead of 54 °C) to reveal potential, subtle alterations that may occur in basal thermal nociception. Reaction times (s) were measured with a stopwatch immediately before morphine or vehicle or saline administration and 15, 30 and 45 min after; each treatment was blind to the experimenter. The endpoint for the licking response was the first paw lick whether it was lick of the front or rear paw. Those mice scoring less than 12 and more than 18 s in the pretest were rejected. All treatments for a same experiment were performed on the same period of time. All the experiments were performed at the same hours (9–13 a.m.). Mice were randomly assigned to each group. Dose–response experiments were done using independent groups.

2.7. Controls

The mice which underwent the hot plate test were submitted to paw temperature measurement 24 h, 10 and 1 min before estimation of hot plate latency. The temperature was measured with an infrared thermometer (Omega, Stanford, CT). At the conclusion of the experiments, the mice were anesthetized, their brains were excised and cut coronally to check the visible path of i.c.v. injection. Only data from mice in which the injection was correctly located within ventricles were considered.

2.8. Motor coordination

Groups of mice pretreated with all the used drugs or ODNs at the highest doses used in the above experiments were submitted to rota-rod (Vaught et al., 1985) and hole-board (Ghelardini et al., 2002) behavioural tests.

2.9. Western blot analysis

Western blot analysis was performed as previously described in detail (Pan et al., 1995). In summary, membrane homogenates (1 μg/μl protein) from different brain regions of aODN, dODN, mODN and vehicle pretreated mice were solubilized in SDS buffer and separated on 10% polyacrylamide gels (1.5 mm). Proteins were transferred to nitrocellulose (1.5 h at 190 mA) and the membranes were blocked in PBS containing 3% BSA for 1 h before addition of primary antisera. Sc403 (PLCβ$_3$), sc-211 (PKCγ) and Sc-5274 (β-tubulin) (Santa Cruz Biotechnology, Santa Cruz, USA) were used as probes at 1:1000 dilution. The blotting was visualized using a chemiluminescence detection system (Pierce Biotechnology Inc., Rockford, IL, USA) and quantified with the Versa Doc 1000 Imaging System (Bio-Rad Laboratories, Hercules, CA, USA). Protein was determined as Lowry method (Lowry et al., 1951) using BSA as standard. Samples from the same brain region of aODN, dODN, mODN and vehicle treated mice were processed simultaneously in the same gel. Each experiment was repeated three times at the same protein concentration. The differences observed as density average values corresponding to aODN and mODN treated mice were expressed as a percentage.

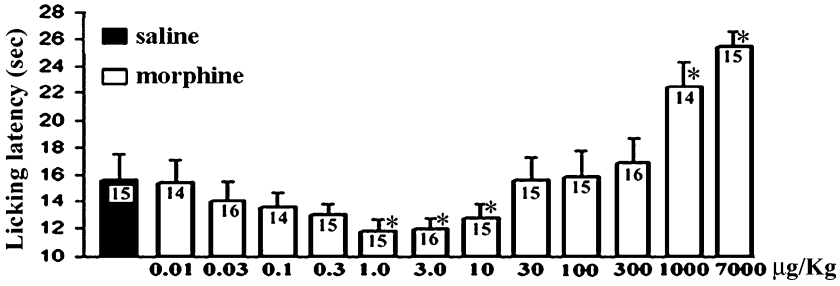

Fig. 2. Effect of increasing morphine doses on the licking latency response in the hot plate test. The licking latency values were measured 15, 30 and 45 min after s.c. morphine administration (0.01–7000 μg/kg). The values reported in figure are at 15 min after morphine administration. Vertical bars represent SEM and *$\alpha < 0.05$ in comparison with saline treated value. The number reported on the top of bar graph represents the number of animals used in each experiment.

2.10. Statistical analysis

All experimental results were given as means ± SEM. Analysis of variance ANOVA, followed by Fisher's protected least significant difference procedure for post hoc comparison, was used to verify significance between two means of behavioural results. Data were analyzed with the StatView software for the Macintosh (1992). A significance level (α) less than 0.05 was considered significant.

2.11. Data analysis

The percentage of maximum possible effect (%MPE) was calculated for each mouse at each dose and time point according to the following formula:

$$\%\text{MPE} = \frac{(\text{postreatment latency} - \text{pretreatment latency})}{(\text{cutoff latency} - \text{pretreatment latency})} \times 100,$$

where licking latency was measured in seconds and cutoff latency was selected at 30. The trapezoidal rule, without extrapolation to infinite time, was used to calculate area under the %MPE versus time curves (AUCs) for each individual animal.

3. Results

3.1. Dose–response curve of morphine in hot plate test

Morphine s.c. administered at different doses (0.01–7000 μg/kg) induced a bimodal response in the hot plate test (Fig. 2). The maximum hyperalgesic effect was reached at 1–10 μg/kg; this effect appeared 15 min after administration and persisted almost unchanged up to 45 min and then diminished. Doses ranging between 30 and 300 μg/kg were devoid of any effect on mice nociceptive threshold, whereas, at a dose of 1–7 mg/kg, morphine induced analgesia. Naloxone administration completely reversed the hyperalgesic effect whereas naloxone methiodide administration lacked to reverse the hyperalgesic effect (Table 1). The μOR antagonist CTOP and μOR_1 selective antagonist naloxonazine completely reversed the 1 μg/kg morphine hyperalgesic effect whereas the δ_1 antagonist BNTX, the δ_2 antagonist naltriben and the κ antagonist nor-NBI failed to reverse the hyperalgesic effect (Table 1). The same treatments, when administered alone, did not modify the licking latency of mice in comparison with saline administered animals (data not shown).

3.2. Cyclic AMP and DAG determination

The administration of forskolin at different concentrations (0.03–0.06 μg/kg i.c.v.) did not modify the licking latency response in the morphine hyperalgesic dose treated mice compared to forskolin untreated mice (data not shown). Acute administration of morphine at analgesic dose (7 mg/kg) significantly decreased cAMP levels in different mouse brain areas in comparison with saline

Table 1
Effect of different opioid antagonist pretreatment on licking latency at 15, 30 and 45 min after 1 μg/kg s.c. morphine administration

Treatment	Before	15 min after	30 min after	45 min after
Saline	15.4 ± 0.7	14.9 ± 1.0	14.8 ± 0.9	15.6 ± 0.9
MF (1 μg/kg)	15.1 ± 0.5	12.1 ± 0.6^	12.4 ± 0.7^	14.5 ± 0.7
MF + naloxone (2 mg/kg)	14.4 ± 0.7	15.1 ± 0.5	15.4 ± 0.6	15.1 ± 0.8
MF + naloxone methiodide (4.7 mg/kg)	15.5 ± 0.9	12.4 ± 1.1^	12.9 ± 0.7^	15.0 ± 0.7
MF + CTOP (0.001 μg/mouse i.c.v.)	14.7 ± 0.7	14.9 ± 1.0	15.2 ± 0.9	15.0 ± 0.8
MF + naloxonazine (1 μg/mouse i.c.v.)	14.9 ± 0.9	15.1 ± 1.1	15.0 ± 0.8	15.8 ± 0.7
MF + naltriben (19 μg/mouse i.c.v.)	15.7 ± 1.2	12.1 ± 0.5^	12.9 ± 0.9^	14.3 ± 0.7
MF + BNTX (3.5 μg/mouse i.c.v.)	14.7 ± 0.8	12.8 ± 0.7^	12.9 ± 0.9^	15.2 ± 1.0
MF + nor-NBI (735 μg/mouse i.c.v.)	15.4 ± 0.6	12.2 ± 0.6^	12.8 ± 0.9^	14.9 ± 0.8

MF, morphine (1 μg/kg); before, before MF administration; ^$\alpha < 0.05$ versus saline.

Table 2
Cyclic AMP and DAG level determined in different regions from mouse brain at different times after morphine or saline s.c. treatment

Treatment	C	S	HP	PAG
cAMP (fM/mg protein)				
Saline (15 min)	14.0 ± 0.7	9.6 ± 0.3	18.4 ± 1.2	10.2 ± 0.5
Morphine (15 min) (1 μg/kg)	14.5 ± 0.4	10.1 ± 0.4	19.1 ± 0.9	11.0 ± 0.7
Morphine (30 min) (1 μg/kg)	16.1 ± 2.1	9.4 ± 0.7	16.7 ± 1.1	12.1 ± 1.3
Morphine (15 min) (7 mg/kg)	5.2 ± 0.1^	4.6 ± 0.3^	7.9 ± 0.3^	6.0 ± 0.1^
DAG (nM/g protein)				
Saline	50 ± 4.1	38 ± 3.9	54 ± 3.4	62 ± 5.1
Morphine (15 min) (1 μg/kg)	96 ± 7.3^	41 ± 4.9	83 ± 4.9^	103 ± 5.2^
Morphine (15 min) (7 mg/kg)	65 ± 11	37 ± 5.6	62 ± 9.8	74 ± 12
Morphine (30 min) (7 mg/kg)	122 ± 16^	44 ± 5.1	99 ± 8.2^	168 ± 14^

Measurement times are reported in brackets. Each value is the mean of three independent experiments. ^$\alpha < 0.05$ versus saline. C, cerebral cortex; S, striatum; HP, hippocampus; PAG, periaqueductal grey matter.

(Table 2). The cAMP levels were not affected by morphine treatment at hyperalgesic dose (1 μg/kg) when compared with saline administration (Table 2). A significant increase of DAG occurred in cortex, periaqueductal grey matter and hippocampus brain areas from mice administered with morphine hyperalgesic dose compared with saline administered animals whereas striatal region did not show a significant increase in DAG level in presence of low dose morphine administration to mice (Table 2). DAG level after analgesic morphine dose administration did not show any significant increase with respect to saline control at 15 min after morphine administration whereas a significant increase appeared at 30 min after (Table 2). The DAG increase lasted for 45 min (data not shown).

3.3. Effect of PLC and PKC inhibitors on morphine-induced hyperalgesia

The PLC inhibitor U73122 dose dependently prevented the thermal hypernociception induced by morphine (1 μg/kg) in the mouse hot plate test (Fig. 3a). The reversal of the hyperalgesic effect appeared 15 min after administration and persisted almost unchanged up to 30 min and then diminished. By contrast, U73343, an inactive analog of U73122 and used as a negative control, did not alter the reaction of pain threshold produced by the hyperalgesic morphine dose (Fig. 3b). Pretreatment with the PKC blocker calphostin C produced a dose-dependent inhibition of 1 μg/kg morphine-in-

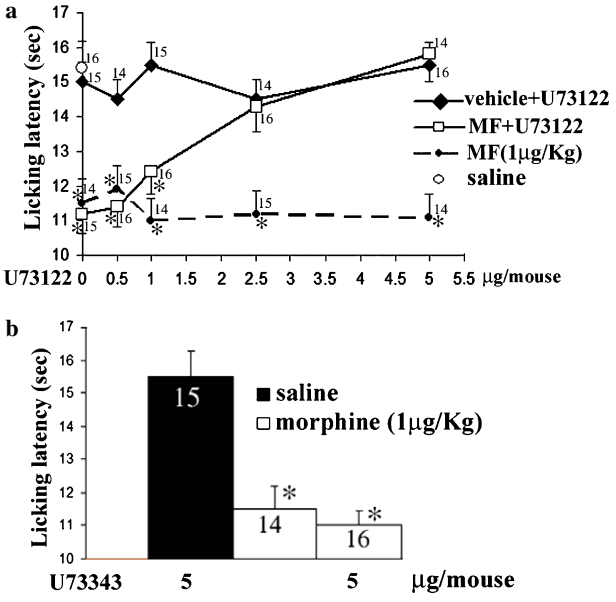

Fig. 3. Reversal of morphine-induced hyperalgesia by pretreatment with U73122 at different doses (a) and U73343 (5 μg/mouse) (b). The licking latency values of hot plate test were measured before and 15, 30 and 45 min after 1 μg/kg s.c. morphine administration. The results are represented in figure at 15 min after morphine administration. MF, morphine. Vertical bars represent SEM and *$\alpha < 0.05$ in comparison with saline or vehicle treated value. The number reported on the top of bar graph or nearby data plot represents the number of animals used in each experiment.

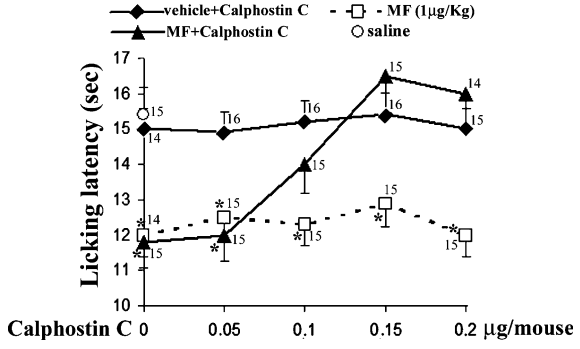

Fig. 4. Reversal of morphine-induced hyperalgesia by pretreatment with Calphostin C at different doses. The licking latency values of hot plate test were measured before and 15, 30 and 45 min after 1 μg/kg s.c. morphine administration. The results are represented in figure at the time of the maximum effect induced by pretreatment (15 min after morphine administration). MF, morphine. Vertical bars represent SEM and *$\alpha < 0.05$ in comparison with saline or vehicle treated value. The number reported on data plot represents the number of animals used in each experiment.

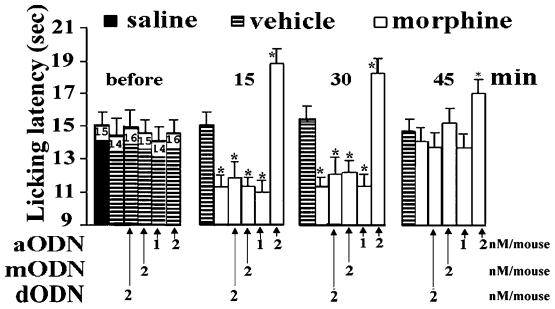

Fig. 5. Effects of aODN, dODN and mODN against PLCβ$_3$ on hyperalgesia induced by 1 μg/kg s.c. morphine administration. Licking latencies were measured before morphine administration and 15, 30, and 45 min after. Vertical bars represent SEM and *$\alpha < 0.05$ in comparison with saline or vehicle treated value. The number reported on the top of bar graph represents the number of animals used in each experiment.

duced hyperalgesia in the hot plate test (Fig. 4). The reversal of the hyperalgesic effect appeared 15 min after administration, slightly decreased 30 min after and then diminished. All the compounds used in pretreatments, injected alone, produced neither a hyperalgesic nor an analgesic effect (Figs. 3 and 4).

3.4. Effect of PLCβ$_3$ and PKCγ downregulation on morphine-induced hyperalgesia

The thermal hypernociception induced by morphine was prevented by pretreatment with the aODN against PLCβ$_3$, at 2 nmol/mouse (Fig. 5). 1 nmol/mouse was ineffective; 2 nmol/mouse prevented the morphine-induced hypernociception, whereas it mildly increased the nociceptive threshold (Fig. 5). Higher doses of PLCβ$_3$ aODN could not be administered because this was lethal. Pretreatment with aODN against the PKCγ isoform (0.5–3 nmol/mouse) prevented the hyperalgesia induced by low dose morphine (1 μg/kg) in a dose-dependent manner (Fig. 6). Lower aODN doses (0.5–1 nmol/mouse) were ineffective in modifying the hyperalgesic effect whereas higher doses (2–3 nmol/mouse) prevented the hyperalgesic response revealing a mild analgesic effect. Mismatch ODNs and dODNs against both isoenzymes, when used at the higher doses in presence or absence of morphine hyperalgesic dose, did not significantly modify the nociceptive threshold in hot plate test with respect to morphine or vehicle administered animals (Figs. 5 and 6). The area under curves of average percent maximum possible effect (%MPE) versus time for morphine in aODN treated mice, linearly increased with respect to PLCβ$_3$ and PKCγ aODN doses (Fig. 7). The prevention of morphine hyperalgesia produced by aODNs against PLCβ$_3$ and PKCγ at highest active doses disappeared 7 days after the end of the aODN pretreatment (data not shown).

3.5. Immunoblotting

Immunoblotting revealed a significant decrease of PLCβ$_3$, PKCγ expression, respectively, in different brain areas from mice previously treated with corresponding aODNs with respect to mODN treated mice (Fig. 8; Table 3). Immunoblot was re-probed for a non-regulatory protein, β-tubulin, and no significant density difference was revealed for this protein between samples from the PLCβ$_3$ and PKCγ downregulated brain regions (data not shown).

3.6. Effect of NMDA receptor antagonists on hyperalgesia

The administration of site-specific NMDA receptor antagonist MK801 and ketamine to mice completely reversed the hyperalgesic effect induced by 1 μg/kg morphine (Fig. 9). Pretreatment with MK801 at 0.005–0.3 μg/mouse produced a dose-dependent inhibition of 1 μg/kg morphine-induced hyperalgesia in the hot plate test (Fig. 9a). At the highest MK801 dose, the reversion of the hyperalgesic effect appeared 15 min after administration, slightly decreased 30 min after and then diminished. Pretreatment with ketamine at 0.05–0.5 μg/mouse produced a dose-dependent inhibition of 1 μg/kg morphine-induced hyperalgesia in the hot plate test (Fig. 9b). At the highest ketamine dose,

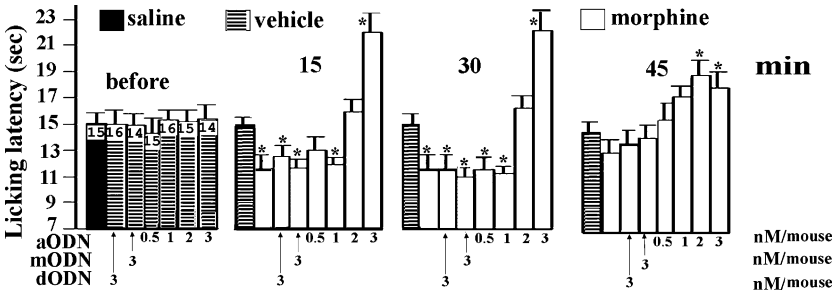

Fig. 6. Effects of aODN, dODN and mODN against PKCγ on hyperalgesia induced by 1 μg/kg morphine administration. Licking latencies were measured before morphine administration and 15, 30, and 45 min after. Vertical bars represent SEM and *$\alpha < 0.05$ in comparison with saline or vehicle treated value. The number reported on the top of bar graph represents the number of animals used in each experiment.

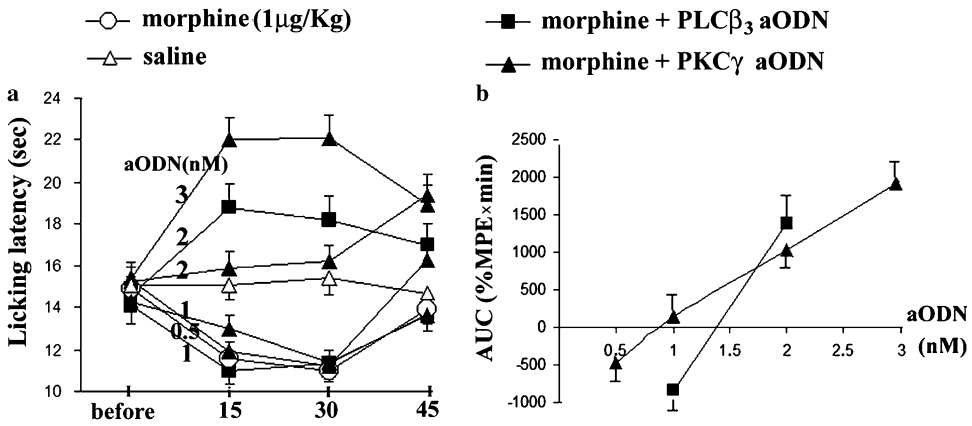

Fig. 7. Area of %MPE versus time curves for aODN tested in morphine-induced hyperalgesia. Licking latency versus time curves in hot plate test after saline, 1 μg/kg morphine administration in mice or 1 μg/kg morphine administration in PLCβ$_3$ and PKCγ aODN treated mice are plotted in (a). Areas under the average percent maximum licking latency effect (%MPE) versus time curves (AUCs) are represented in (b) for aODN treatment at different doses in presence of 1 μg/kg morphine dose. Vertical bars represent SEM.

the reversion of the hyperalgesic effect appeared 15 min after administration, almost unchanged 30 min after and then diminished. All the compounds used in pretreatments, injected alone, produced neither a hyperalgesic nor an analgesic effect (data not shown).

3.7. Effect of PLCβ$_3$ and PKCγ downregulation on morphine-induced analgesia

In PLCβ$_3$ pretreated mice the analgesic effect induced by 7 mg/kg morphine dose was significantly potentiated at 15 and 30 min after morphine administration (Fig. 10). In PKCγ pretreated mice, the potentiation of the analgesic effect induced by 7 mg/kg morphine dose started at 30 min and was prolonged until 45 min after morphine administration. When an analgesic morphine dose (7 mg/kg) was administered to mice pretreated with aODNs against PLCβ$_3$ and PKCγ at the effective doses, a 46% and 67% increase in the analgesic response, respectively, was induced in comparison with aODN untreated animals, as shown by area under average percent maximum possible effect (%MPE) versus time course (AUC) (Fig. 11).

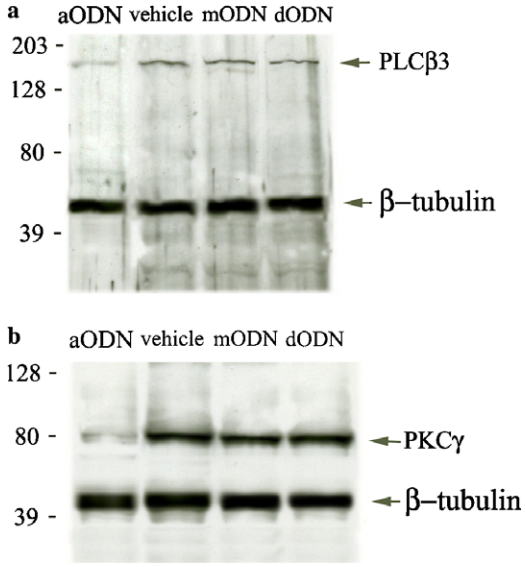

Fig. 8. Immunoblots of PLCβ$_3$ or PKCγ downregulated mouse brain. Brain PAG from PLCβ$_3$ or PKCγ aODN, mODN, dODN at the highest dose (2 and 3 nM/mouse) and vehicle pretreated mice were revealed for PLCβ$_3$ (a) and PKCγ (b). The molecular weight markers (kDa; Bio-Rad) are indicated on the left.

3.8. Effect of treatments on mouse behavior

The endurance time on the rotating rod, evaluated before and 15, 30 and 45 min after 1 μg/kg morphine administration, indicated a lack of any impairment in the motor coordination of animals pretreated with drugs and ODNs at the same time administration and doses (data not shown). The spontaneous motility as well as the inspection activity of mice, expressed as counts in 10 min, was unmodified by the above-mentioned compounds in comparison with the corresponding control group (data not shown). The skin temperature of the mice paws remained unchanged after administration of the different pretreatments (data not shown) showing that these compounds do not induce any significant change in basal temperature.

Table 3
Percent decrease of the density values revealed by immunoblotting from PLCβ$_3$ and PKCγ aODN treated versus mODN treated mice was computed for each brain region

Brain region aODN	C	S	HP	PAG
PLCβ$_3$	66 ± 9	–	70 ± 11	82 ± 9
PKCγ	63 ± 7	74 ± 8	65 ± 8	78 ± 10

Density value obtained from mODN treated mice was assumed as 100%. Values are means ± SEM from three independent experiments. C, cerebral cortex; S, striatum; HP, hippocampus; PAG, periaqueductal grey matter; –, not detectable.

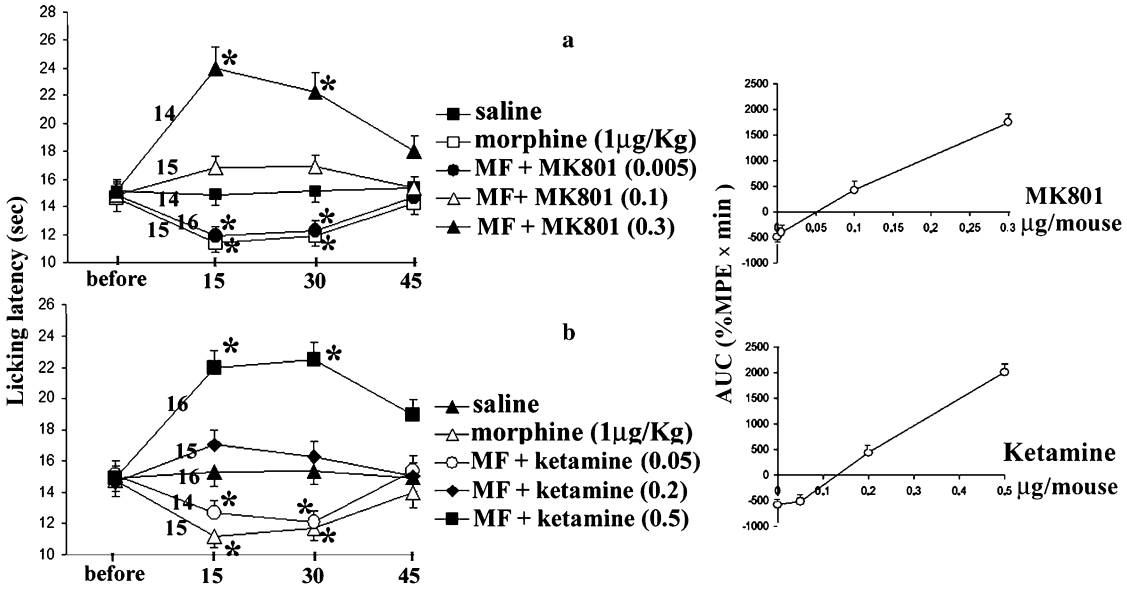

Fig. 9. Effect of pretreatment with NMDA antagonists on morphine-induced hyperalgesia. Plotting of licking latency versus time curves in hot plate test after saline or morphine (1 μg/kg) administration in untreated mice or 1 μg/kg morphine (MF) administration in mice pretreated with MK801 (0.005–0.3 μg/mouse i.c.v.) and ketamine (0.05–0.5 μg/mouse i.c.v.) is represented on left side. Areas under the average percent maximum licking latency effect (%MPE) versus time curves (AUCs) are represented for NMDA antagonists tested in morphine-induced hyperalgesia on right side. Vertical bars represent SEM and $*\alpha < 0.05$ in comparison with saline treated value. The number reported on data plot represents the number of animals used in each experiment.

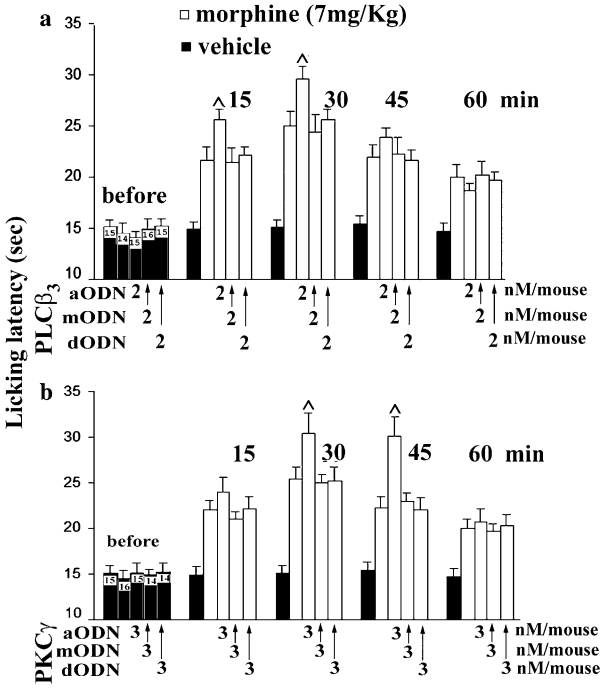

Fig. 10. Effects of aODN, dODN and mODN against $PLC\beta_3$ (a) and PKCγ (b) on analgesia induced by 7 mg/kg s.c. morphine administration. Licking latencies were measured before morphine administration and 15, 30, 45 and 60 min after. $\hat{}\alpha < 0.05$ in comparison with 7 mg/kg morphine dose. Vertical bars represent SEM. The number reported on the top of bar graph represents the number of animals used in each experiment.

4. Discussion

The present study confirms that low dose morphine systemic administration induced hyperalgesia in normal mice submitted to a condition of acute thermal nociception. The hyperalgesic effect was reached at 1–10 μg/kg subcutaneous morphine administration, as demonstrated by the significant decrease in nociceptive threshold. This effect was completely reversed by the administration of naloxone. The CNS origin of low dose morphine hyperalgesia was shown because the hyperalgesia was completely blocked by naloxone, which crosses BBB, and not by naloxone methiodide, administered at a dose which blocks the peripheral effects of morphine in rodents but does not cross the BBB. The effect of naloxone was reproduced using the selective μOR antagonist CTOP and μOR_1 antagonist naloxonazine but not the δ-opioid receptor antagonists naltriben and BNTX, or the κ-opioid receptor antagonist nor-NBI administered at effective doses. These data demonstrate that the hyperalgesic effect is mediated by a specific opiate receptor subtype, i.e., μOR_1.

Cyclic AMP levels measured at the time of the maximum hyperalgesic effect in mice previously administered with 1 μg/kg morphine dose did not significantly change with respect to control mice whereas, as expected, cAMP values significantly decreased in mice administered with morphine at the analgesic dose. Administration of forskolin, an adenylate cyclase activator, at a dose which increases cAMP level in rodents, did not significantly modify the hyperalgesic effect. These

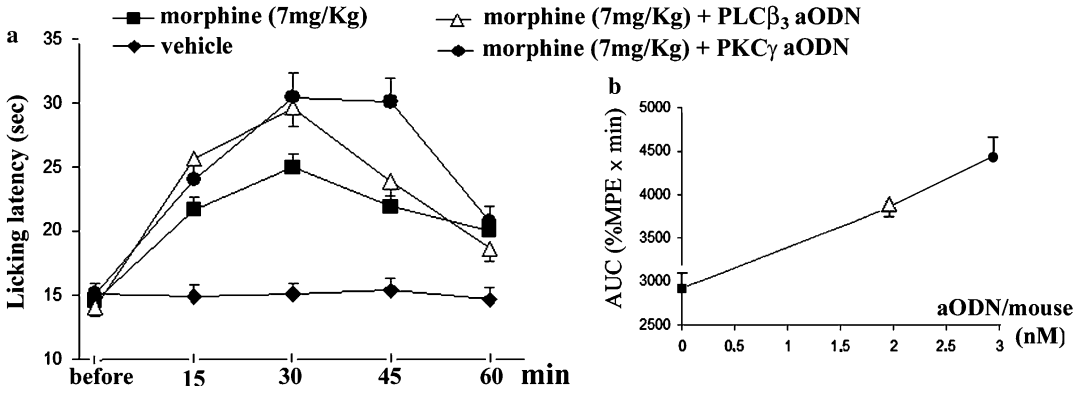

Fig. 11. Areas under the average percent maximum licking latency effect (%MPE) versus time curves (AUCs) for aODNs tested in morphine-induced analgesia. Licking latency versus time curves in hot plate test after vehicle or morphine (7 mg/kg) administration in untreated mice or 7 mg/kg morphine administration in PLCβ_3 (2 nM/mouse) and PKCγ (3 nM/mouse) aODN treated mice are plotted in (a). Areas under %MPE versus time curves (AUCs) are represented in (b) for each treatment. Vertical bars represent SEM.

data did not suggest that stimulatory effect induced by morphine low dose administration in vivo was due to cAMP stimulation.

In our experiments, the administration of the non-selective isoform PLC inhibitor U73122 to mice dose dependently prevented the hyperalgesia induced by low dose morphine exposure. By contrast U73343, a succinimido analog used as negative control for U73122 and a weak PLC inhibitor failed to reverse the hyperalgesia. Thus, morphine-induced hyperalgesia appeared to be mediated by PLC activation. Among the PLCβ isoforms, the downregulation of PLCβ_3 isoenzyme in mouse brain by anti-PLCβ_3 aODN pretreatment induced a reversion of low dose morphine stimulated hyperalgesic effect, which was mildly antinociceptive at the highest anti-PLCβ_3 aODN dose. Control experiments excluded toxicity and hybridization-dependent artefacts. Considering that PLC stimulates PKC in PLC/PKC inositol-lipid signaling pathway, the activation of PKC was also investigated. This hypothesis was supported by the increase in value of DAG, a product of PLCβ, obtained in different brain regions of mice administered with morphine hyperalgesic dose with respect to saline administered mice. Pretreatment with calphostin C, a selective PKC inhibitor, dose dependently prevented the hyperalgesia induced by morphine. These findings suggest that activation of PKC constitutes a significant step in morphine-induced hyperalgesia. In particular, PKCγ appears to participate in increased pain sensitivity (Malmberg et al., 1997; Martin et al., 2001; Celerier et al., 2004). We further demonstrated that the downregulation of PKCγ in mouse brain by anti-PKCγ aODN pretreatment induced a reversal of morphine hyperalgesic effect in mice and, at the same time, a mild analgesic effect. Control experiments excluded toxicity and hybridization-dependent artefacts.

Furthermore, μOR stimulation triggers the activation of NMDA receptors by increasing intracellular PKC activity (Chen and Huang, 1991) as well as translocation of the cytosolic PKCγ to the plasma membrane leading to phosphorylation of the NMDA receptors implicated in pain promotion (Suen et al., 1998). Evidence for NMDA receptor activation during the hyperalgesic response to low dose morphine administration was recently demonstrated (Holtman and Wala, 2005). In our behavioural test, low dose morphine-induced hyperalgesia was prevented by NMDA high affinity, non-competitive antagonist MK801 and ketamine. This effect was dose dependent. PKCγ associates physically with NMDA NR1 subunit in the postsynaptic density in rat brain, suggesting that these receptors may be directly phosphorylated by the kinase, leading to enhancement of synaptic activity (Suen et al., 1998). The majority of NMDA NR1 labeled dendrites contained μOR labeling in ventrolateral PAG (Commons et al., 1999), a supraspinal brainstem region of interest because of its established role in modulation of nociceptive transmission. This area was found PKCγ and PLCβ_3 positive in our immunoblotting experiments. Cortex electrical stimulation produced significant decrease in tail flick latency (Calejesan et al., 2000), suggesting that cortical areas support the descending facilitatory modulation of nociceptive response. NMDA receptors in anterior cingulated cortex are involved in descending facilitation through a relay in the rostral ventromedial medulla (RVM) (Calejesan et al., 2000; Zhang et al., 2005). The hippocampal formation, a high density μOR area, has been involved in affective-motivational response to noxious-aversive events. Microinjection of a glutamate receptor antagonist into the dorsal hippocampal formation of the rat attenuated the nociceptive behavior to the unconditioned hind paw injection of the algogen formalin (McKenna and Melzack, 2001). Both PLCβ_3 and PKCγ could be detected by immunoblotting in cortical and hippocampal areas. Otherwise, PLCβ_3 was not revealed by our immunoblotting in striatum. Therefore,

we surmise that this area is not implicated in circuits for low dose morphine-induced hyperalgesia. PKCγ was expressed in very few of the μOR positive cells in the spinal cord in absence of stimulus, suggesting that this isoform does not underlie the interaction between μOR and NMDA receptors at spinal level (Zeitz et al., 2001). Otherwise, PKCγ immunoreactivity increased in spinal cord after chronic morphine administration and was prevented by NMDA antagonist administration (Mao et al., 1995).

Pronociceptive actions are promoted by the PAG/RVM circuit (Basbaum and Fields, 1984), classically involved in antinociception, depending on the intensity of the triggering stimulus (Lima and Almeida, 2002). Facilitation of the nociceptive response capacity mediated by RVM, a brainstem area receiving projections from PAG, is triggered by much less intense local chemical or electrical stimulation than that resulting on inhibition (Zhuo and Gebhart, 1997). We surmise that the PAG/RVM circuit acts at supraspinal level, inducing hyperalgesia through the nociceptive PLCβ$_3$/PKCγ/NMDA pathway stimulated by low doses of morphine, through μOR$_1$ receptor, in mouse brain. Otherwise, a different molecular pathway of bimodal excitatory/inhibitory action induced by opioid agonists on dorsal root ganglionic sensory neurons was proved, suggesting that different types of mechanism act depending on nervous system areas. Strong evidence indicates that opioid receptor can be interconverted rapidly between inhibitory G$_{i/o}$ coupled and excitatory (G$_s$ coupled) mode, following physiological alterations in the concentration of cAMP/PKA-dependent glycolipid GM1 ganglioside in neuronal sensory cell membranes (Crain and Shen, 1998, 2000, 2004).

The PLCβ$_3$/PKCγ pronociceptive-signaling pathway appears to play an opposing role in morphine analgesia. When mice were treated with a morphine analgesic dose (7 mg/kg), the downregulation of PLCβ$_3$ or PKCγ at the same aODN doses used for the prevention of the hyperalgesic effect induced a potentiation in analgesic response. The magnitude of difference in morphine-induced analgesia was dramatically greater in PLCβ$_3$/PKCγ downregulated mice (AUC 46% and 67%, respectively, greater in aODN treated compared with untreated mice). The potentiation of the analgesic effect was observable at the earlier time and, in PKCγ downregulated mice, lasted longer. These results suggest that increased morphine-induced analgesia observed in the PLCβ$_3$ or PKCγ aODN treated mice does not result from a true potentiating effect of PLCβ$_3$ or PKCγ downregulation, rather to the blockade of the pain facilitatory system activated by these enzymes.

Dual effects have been encountered in postoperative pain management by opioids. Hyperalgesia and allodynia have been observed in human volunteers after opiod analgesia (Guignard et al., 2000; Angst et al., 2003; Compton et al., 2003). This paradoxical effect was usually ascribed to progressive reduction of opioid effects, occurring over a period of weeks, with repeated drug administration (tolerance) or following a single opiate administration (short-term tolerance). Hyperalgesia is apparent both immediately after administration of a low (1–10 μg/kg) dose of morphine to mice or, at a later time, after analgesic morphine dose administration when the opiate concentration is expected to be as low as morphine brain concentration after low dose administration (Glare and Walsh, 1991). The hyperalgesic effect has typically been observed as a delayed response seen subsequent to the analgesic response produced by central or systemic administration of opioid agonists (Celerier et al., 2000; Mao, 2002; Richebe et al., 2005). Therefore, tolerance – especially short-term tolerance – may be not mainly due to a decrease in opioid effectiveness, as conventionally described, but might result from the expression of nociceptive facilitatory systems which, at later times after morphine analgesic dose administration, are not overwhelmed by the opponent antinociceptive inhibitory systems. The conventional practice of opioid therapy in presence of diminishing analgesic efficacy in the perioperative setting is based on a dose escalation to restore analgesic effects, assuming the development of opioid short-term tolerance. Otherwise, morphine decreased efficacy may be ascribed to paradoxical opioid-induced pain sensitivity. We surmise that the clinical management of pain by morphine can be revisited in light of the identification of the signaling molecules of the hyperalgesic pathway. New strategies are needed to reduce opioid-induced pain sensitivity such as a combined use of morphine and clinically available inhibitors of the pronociceptive system.

References

Abbott FV, Franklin KB, Connell B. The stress of a novel environment reduces formalin pain: possible role of serotonin. Eur J Pharmacol 1986;126:141–4.

Angst MS, Koppert W, Pahl I, Clark DJ, Schmelz M. Short-term infusion of the mu-opioid agonist remifentanil in humans causes hyperalgesia during withdrawal. Pain 2003;10:49–57.

Basbaum AI, Fields HL. Endogenous pain control systems: brainstem spinal pathways and endorphin circuitry. Annu Rev Neurosci 1984;7:309–38.

Bligh EG, Dyer WJ. A rapid method of total lipid extraction and purification. Can J Biochem Physiol 1959;37:911–7.

Calejesan AA, Kim SJ, Zhuo M. Descending facilitatory modulation of a behavioral nociceptive response by stimulation in the adult rat anterior cingulate cortex. Eur J Pain 2000;4:83–96.

Celerier E, Laulin J, Larcher A, Le Moal M, Simonnet G. Evidence for opiate-activated NMDA processes masking opiate analgesia in rats. Brain Res 1999;847:18–25.

Celerier E, Rivat C, Jun Y, Laulin JP, Larcher A, Reynier P, et al. Long-lasting hyperalgesia induced by fentanyl in rats: preventive effect of ketamine. Anesthesiology 2000;92:465–72.

Celerier E, Laulin JP, Corcuff JB, Le Moal M, Simonnet G. Progressive enhancement of delayed hyperalgesia induced by repeated heroin administration: a sensitization process. J Neurosci 2001;21:4074–80.

Celerier E, Simonnet G, Maldonado R. Prevention of fentanyl-induced delayed pronociceptive effects in mice lacking the protein kinase Cgamma gene. Neuropharmacology 2004;46:264–72.

Chan JS, Lee JW, Ho MK, Wong YH. Preactivation permits subsequent stimulation of phospholipase C by G(i)-coupled receptors. Mol Pharmacol 2000;57:700–8.

Chen L, Huang LY. Sustained potentiation of NMDA receptor-mediated glutamate responses through activation of protein kinase C by a mu opioid. Neuron 1991;7:319–26.

Commons KG, van Bockstaele EJ, Pfaff DW. Frequent colocalization of mu opioid and NMDA-type glutamate receptors at postsynaptic sites in periaqueductal gray neurons. J Comp Neurol 1999;408:549–59.

Compton P, Athanasos P, Elashoff D. Withdrawal hyperalgesia after acute opioid physical dependence in nonaddicted humans: a preliminary study. J Pain 2003;4:511–9.

Crain SM, Shen KF. Modulation of opioid analgesia, tolerance and dependence by Gs-coupled, GM1 ganglioside-regulated opioid receptor functions. Trends Pharmacol Sci 1998;19:358–65.

Crain SM, Shen KF. Antagonists of excitatory opioid receptor functions enhance morphine's analgesic potency and attenuate opioid tolerance/dependence liability. Pain 2000;84:121–31.

Crain SM, Shen KF. Acute thermal hyperalgesia elicited by low-dose morphine in normal mice is blocked by ultra-low-dose naltrexone, unmasking potent opioid analgesia. Brain Res 2001;888:75–82.

Crain SM, Shen KF. Neuraminidase inhibitor, oseltamivir blocks GM1 ganglioside-regulated excitatory opioid receptor-mediated hyperalgesia, enhances opioid analgesia and attenuates tolerance in mice. Brain Res 2004;995:260–6.

Ghelardini C, Galeotti N, Calvani M, Mosconi L, Nicolai R, Bartolini A. Acetyl-L-carnitine induces muscarinic antinociception in mice and rats. Neuropharmacology 2002;43:1180–7.

Glare PA, Walsh TD. Clinical pharmacokinetics of morphine. Ther Drug Monit 1991;13:1–23.

Guignard B, Bossard AE, Coste C, Sessler DI, Lebrault C, Alfonsi P, et al. Acute opioid tolerance: intraoperative remifentanil increases postoperative pain and morphine requirement. Anesthesiology 2000;93:409–17.

Haley TJ, McCormick WJ. Pharmacological effects produced by intracerebral injections of drugs in the conscious mouse. Br J Pharmacol 1957;12:12–5.

Holtman JR, Wala EP. Characterization of morphine-induced hyperalgesia in male and female rats. Pain 2005;114:62–70.

Janecka A, Fichna J, Kruszynski R, Sasaki Y, Ambo A, Costentin J, et al. Synthesis and antinociceptive activity of cyclic endomorphin-2 and morphiceptin analogs. Biochem Pharmacol 2005;9.

Ji D, Sui ZY, Ma YY, Luo F, Cui CL, Han JS. NMDA receptor in nucleus accumbens is implicated in morphine withdrawal in rats. Neurochem Res 2004;29:2113–20.

Jinsmaa Y, Fujita Y, Shiotani K, Miyazaki A, Li T, Tsuda Y, et al. Differentiation of opioid receptor preference by [Dmt1]endomorphin-2-mediated antinociception in the mouse. Eur J Pharmacol 2005;509:37–42.

Kayan S, Woods LA, Mitchell CL. Morphine-induced hyperalgesia in rats tested on the hot plate. J Pharmacol Exp 1971;177:509–13.

Kayser V, Besson JM, Guilbaud G. Paradoxical hyperalgesic effect of exceedingly low doses of systemic morphine in an animal model of persistent pain (Freund's adjuvant-induced arthritic rats). Brain Res 1987;414:155–7.

Laulin JP, Larcher A, Celerier E, Le Moal M, Simonnet G. Long-lasting increased pain sensitivity in rat following exposure to heroin for the first time. Eur J Neurosci 1998;10:782–5.

Laulin JP, Maurette P, Corcuff JB, Rivat C, Chauvin M, Simonnet G. The role of ketamine in preventing fentanyl-induced hyperalgesia and subsequent acute morphine tolerance. Anesth Analg 2002;94:1263–9.

Lee JK, Choi SS, Lee HK, Han KJ, Han EJ, Suh HW. Effects of MK-801 and CNQX on various neurotoxic responses induced by kainic acid in mice. Mol Cells 2002;14:339–47.

Lima D, Almeida A. The medullary dorsal reticular nucleus as a pronociceptive centre of the pain control system. Prog Neurobiol 2002;66:81–108.

Lowry OH, Rosebrough NJ, Farr AL, Randall RJ. Protein measurement with the Folin phenol reagent. J Biol Chem 1951;193:265–75.

Mao J, Price DD, Phillips LL, Lu J, Mayer DJ. Increases in protein kinase C gamma immunoreactivity in the spinal cord of rats associated with tolerance to the analgesic effects of morphine. Brain Res 1995;677:257–67.

Mao J. Opioid-induced abnormal pain sensitivity: implications in clinical opioid therapy. Pain 2002;100:213–7.

Malmberg AB, Chen C, Tonegawa S, Basbaum AI. Preserved acute pain and reduced neuropathic pain in mice lacking PKCgamma. Science 1997;278:279–83.

Martin WJ, Malmberg AB, Basbaum AI. PKCgamma contributes to a subset of the NMDA-dependent spinal circuits that underlie injury-induced persistent pain. J Neurosci 2001;21:5321–7.

McKenna JE, Melzack R. Blocking NMDA receptors in the hippocampal dentate gyrus with AP5 produces analgesia in the formalin pain test. Exp Neurol 2001;172:92–9.

Nestler EJ. Molecular mechanisms of drug addiction. J Neurosci 1992;12:2439–50.

O'Callaghan JP, Holtzman SG. Quantification of the analgesic activity of narcotic antagonists by a modified hot-plate procedure. J Pharmacol Exp Ther 1975;192:497–505.

Pan YX, Cheng J, Xu J, Rossi G, Jacobson E, Ryan-Moro J, et al. Cloning and functional characterization through antisense mapping of a kappa 3-related opioid receptor. Mol Pharmacol 1995;47:1180–8.

Park D, Jhon DY, Lee CW, Lee KH, Rhee SG. Activation of phospholipase C isozymes by G protein beta gamma subunits. J Biol Chem 1993;268:4573–6.

Rady JJ, Takemori AE, Portoghese PS, Fujimoto JM. Supraspinal delta receptor subtype activity of heroin and 6-monoacetylmorphine in Swiss Webster mice. Life Sci 1994;55:603–9.

Rawls SM, Hewson JM, Inan S, Cowan A. Brain delta2 opioid receptors mediate SNC-80-evoked hypothermia in rats. Brain Res 2005;1049:61–9.

Richebe P, Rivat C, Laulin JP, Maurette P, Simonnet G. Ketamine improves the management of exaggerated postoperative pain observed in perioperative fentanyl-treated rats. Anesthesiology 2005;102:421–8.

Rubovitch V, Gafni M, Sarne Y. The mu opioid agonist DAMGO stimulates cAMP production in SK-N-SH cells through a PLC-PKC-Ca^{2+} pathway. Brain Res Mol Brain Res 2003;110:261–6.

Sanchez-Perez AM, Felipo V. Serines 890 and 896 of the NMDA receptor subunit NR1 are differentially phosphorylated by protein kinase C isoforms. Neurochem Int 2005;47:84–91.

Simone DA, Bodnar RJ, Portzline T, Pasternak GW. Antagonism of morphine analgesia by intracerebroventricular naloxonazine. Pharmacol Biochem Behav 1986;6:1721–7.

Smart D, Smith G, Lambert DG. Mu-opioids activate phospholipase C in SH-SY5Y human neuroblastoma cells via calcium-channel opening. Biochem J 1995;15:577–81.

Smart D, Lambert DG. The stimulatory effects of opioids and their possible role in the development of tolerance. Trends Pharmacol Sci 1996;17:264–9.

Steiner AI. Assay of cyclic nucleotides by radioimmunoassay method. Methods Enzymol 1974;38:96–105.

Suen PC, Wu K, Xu JL, Lin SY, Levine ES, Black IB. NMDA receptor subunits in the postsynaptic density of rat brain: expression and phosphorylation by endogenous protein kinases. Brain Res Mol Brain Res 1998;59:215–28.

Suh HH, Tseng LF. Different types of opioid receptors mediating analgesia induced by morphine, DAMGO, DPDPE, DADLE and beta-endorphin in mice. Naunyn Schmiedebergs Arch Pharmacol 1990;342:67–71.

Suh HW, Song DK, Sim YB, Chung KM, Kim YH. Differential effects of forskolin and phorbol-13-myristate injected intrathecally or intracerebroventricularly on antinociception induced by morphine or beta-endorphin administered intracerebroventricularly in the mouse. Neuropeptides 1996;30:177–85.

Tsu RC, Chan JS, Wong YH. Regulation of multiple effectors by the cloned delta-opioid receptor: stimulation of phospholipase C and type II adenylyl cyclase. J Neurochem 1995;64:2700–7.

Van Elstraete AC, Sitbon P, Trabold F, Mazoit JX, Benhamou D. A single dose of intrathecal morphine in rats induces long-lasting hyperalgesia: the protective effect of prior administration of ketamine. Anesth Analg 2005;101:1750–6.

Vaught JL, Pelley K, Costa LG, Setler P, Enna SJ. A comparison of the antinociceptive responses to the GABA-receptor agonists THIP and baclofen. Neuropharmacology 1985;24:211–6.

Wu D, Kang YS, Bickel U, Pardridge WM. Blood–brain barrier permeability to morphine-6-glucuronide is markedly reduced compared with morphine. Drug Metab Dispos 1997;25:768–71.

Zeitz KP, Malmberg AB, Gilbert H, Basbaum AI. Reduced development of tolerance to the analgesic effects of morphine and clonidine in PKC gamma mutant mice. Pain 2001;94:245–53.

Zhang L, Zhang Y, Zhao ZQ. Anterior cingulate cortex contributes to the descending facilitatory modulation of pain via dorsal reticular nucleus. Eur J Neurosci 2005;22:1141–8.

Zhuo M, Gebhart GF. Biphasic modulation of spinal nociceptive transmission from the medullary raphe nuclei in the rat. J Neurophysiol 1997;78:746–58.